

Supporting Information

Mesoporous Co_3O_4 @ Carbon Composites Derived from Microporous Cobalt-Based Porous Coordination Polymers for Enhanced Electrochemical Properties in Supercapacitors

Shuang Wang, Ting Wang, Ying Shi, Guang Liu, and Jinping Li*

Caption of Content

Figure S1. Simulated and experimental powder X-ray diffraction patterns for ZSA-1.

Figure S2. TGA curves of ZSA-1, activated ZSA-1 and Co_3O_4 @ carbon composites.

Figure S3. SEM images for the Co_3O_4 @ carbon composites.

Figure S4. EDX spectrum images of the Co_3O_4 @ carbon composites.

Figure S5. HRTEM images for the Co_3O_4 @ carbon composites.

Figure S6. SEM images for the as-synthesized Co_3O_4 particles.

Figure S7. Specific capacitance versus different charge-discharge current density plots.

Figure S8. Cycling performance of Co_3O_4 @ carbon composites at a current density of $2 \text{ A}\cdot\text{g}^{-1}$.

Figure S9. Cyclic voltammetry curves of ZSA-1 measured at different sweep rates.

Figure S10. Galvanostatic charge-discharge curves of ZSA-1 at different current densities.

Figure S11. Cyclic voltammetry curves of Co_3O_4 particles measured at different sweep rates.

Figure S12. Galvanostatic charge-discharge curves of Co_3O_4 particles at different current densities.

Figure S1. Simulated and experimental powder X-ray diffraction patterns for ZSA-1.

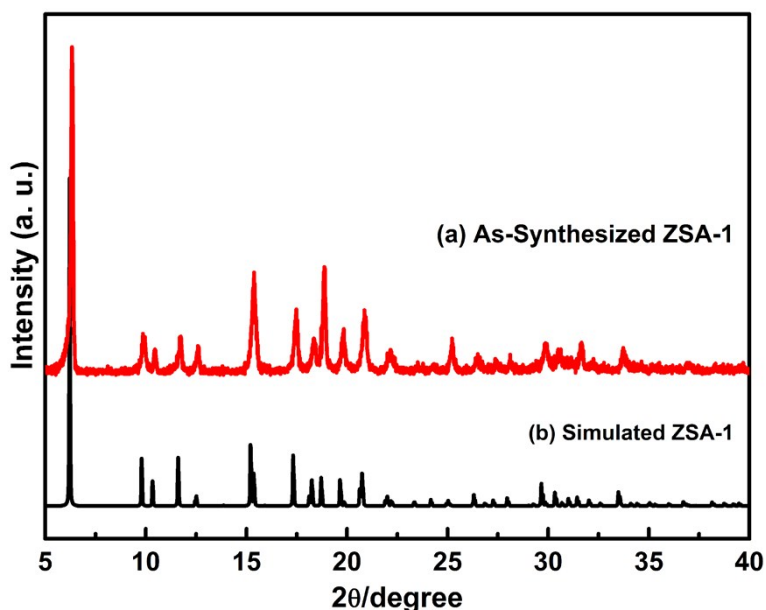
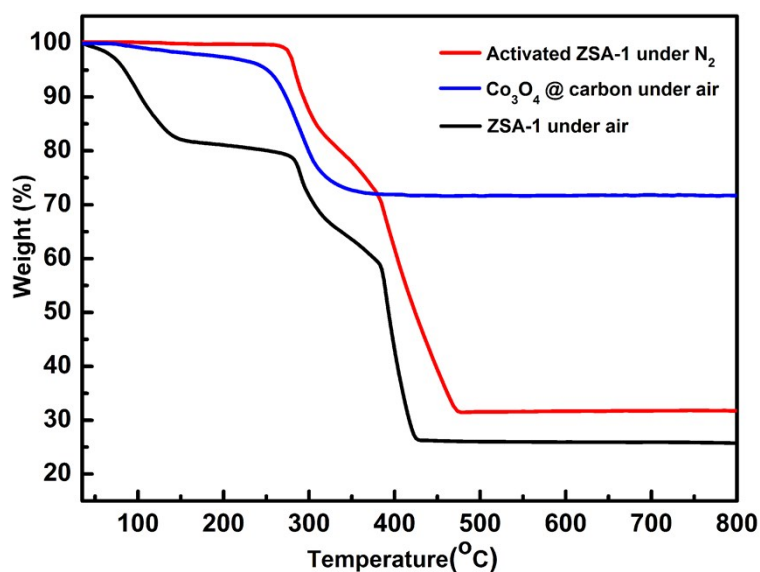


Figure S2. TGA curves of ZSA-1, activated ZSA-1 and Co_3O_4 @ carbon composites.



Thermogravimetric analysis for **ZSA-1** under air shows a weight loss of 18.60 % between 35 and 180°C, corresponding to the loss of guest H_2O molecules, for part of guest H_2O molecules were lost during the sample drying at room temperature. On further heating, a two-step weight loss of 55.7 % between 180 and 430 °C should be correspond to the release of 1, 2-propanediamine and the organic ImDC ligand (calcd: 54.98 %). The residual weight of 26.15 % corresponds to Co_3O_4 .

Figure S3. SEM images for the Co_3O_4 @ carbon composites.

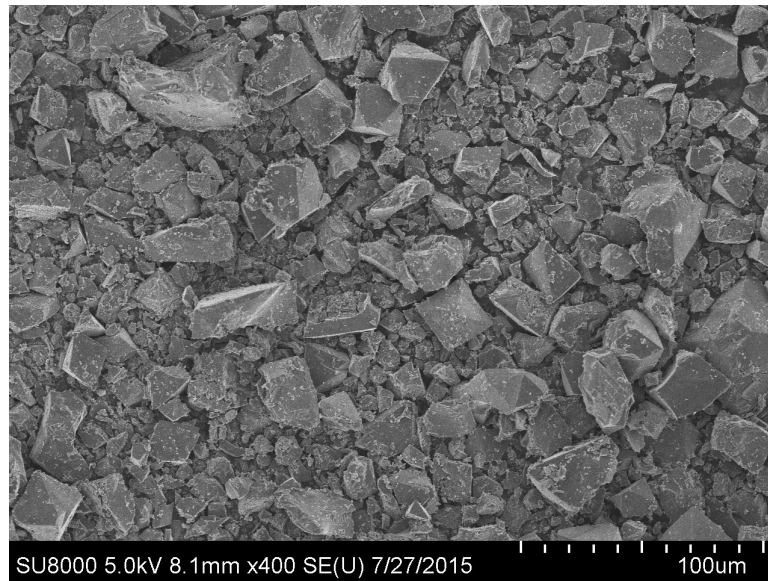


Figure S4. EDX spectrum images of the Co_3O_4 @ carbon composites.

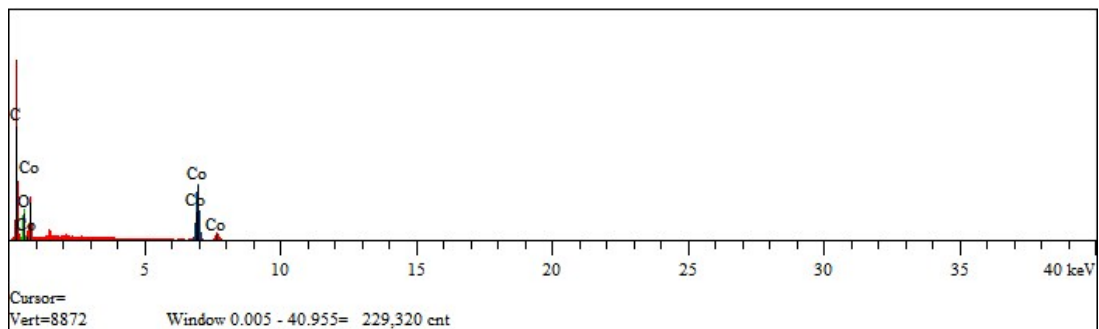


Figure S5. HRTEM images for the Co_3O_4 @ carbon composites.

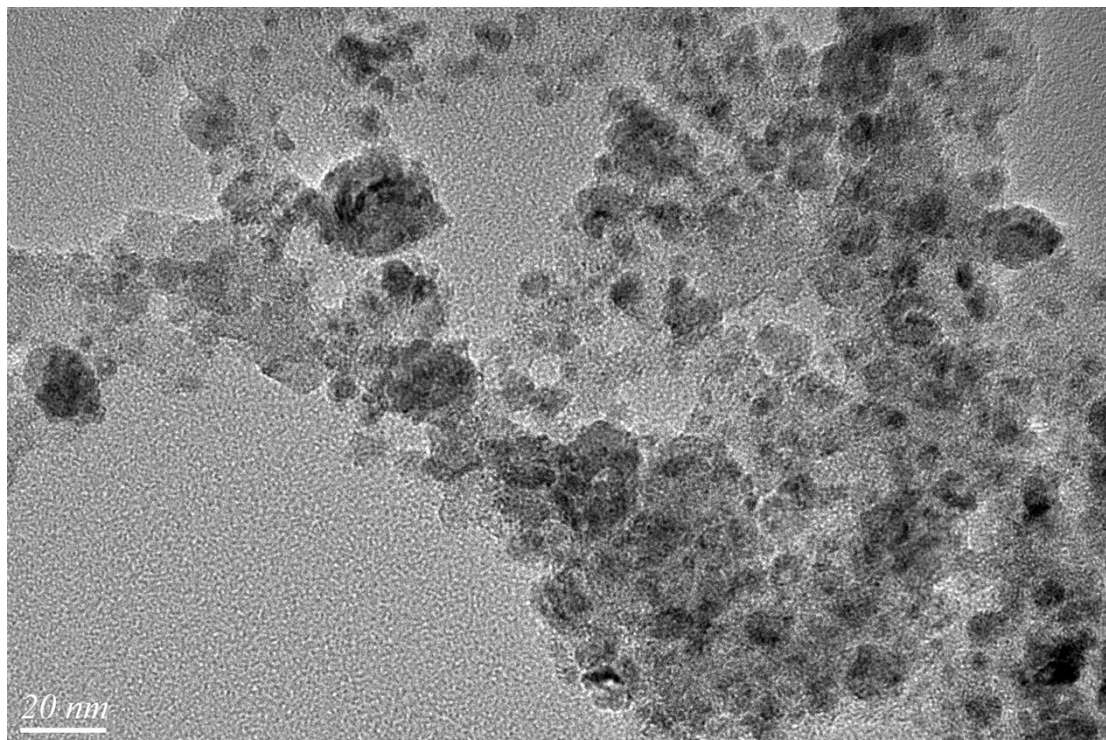


Figure S6. SEM images for the as-synthesized Co_3O_4 particles.

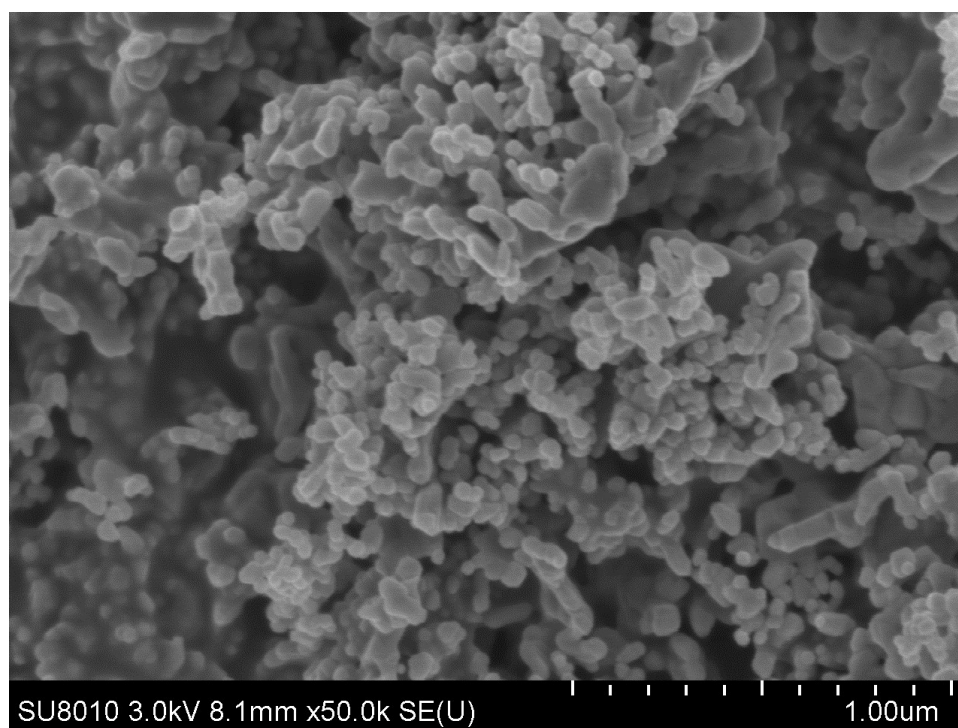


Figure S7. Specific capacitance versus different charge-discharge current density plots.

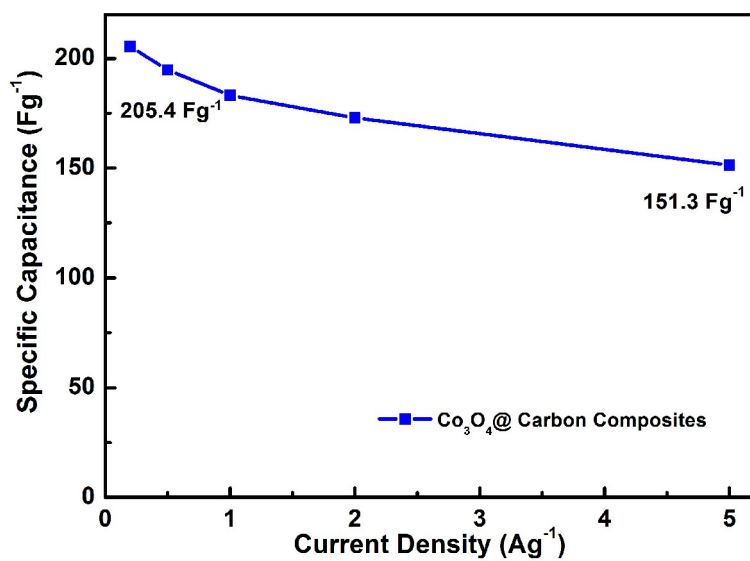


Figure S8. Cycling performance of Co₃O₄ @ carbon composites at a current density of 2 A·g⁻¹.

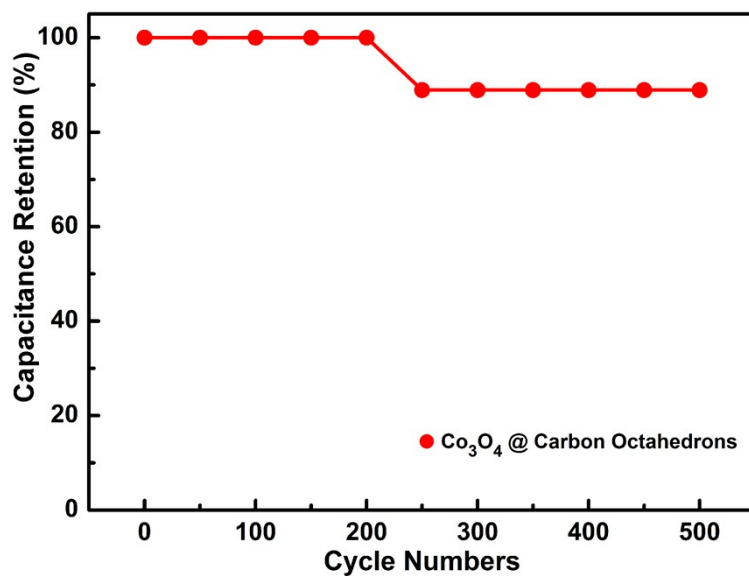


Figure S9. Cyclic voltammety curves of ZSA-1 measured at different sweep rates.

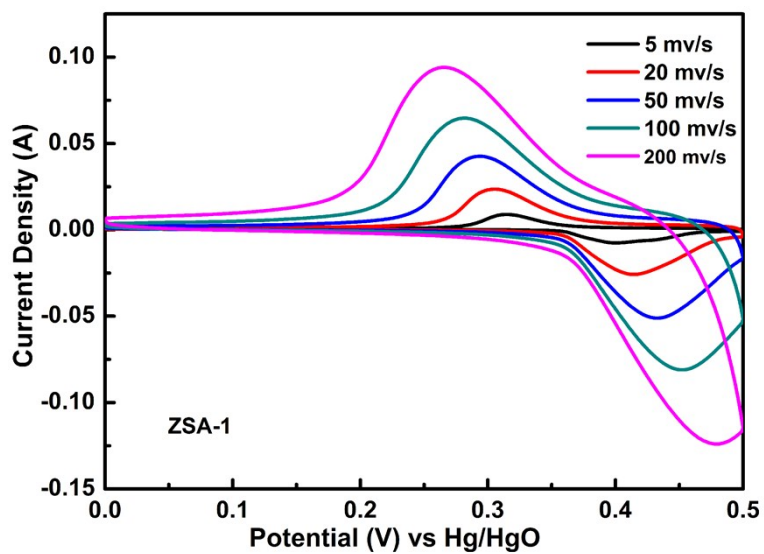


Figure S10. Galvanostatic charge-discharge curves of ZSA-1 at different current densities.

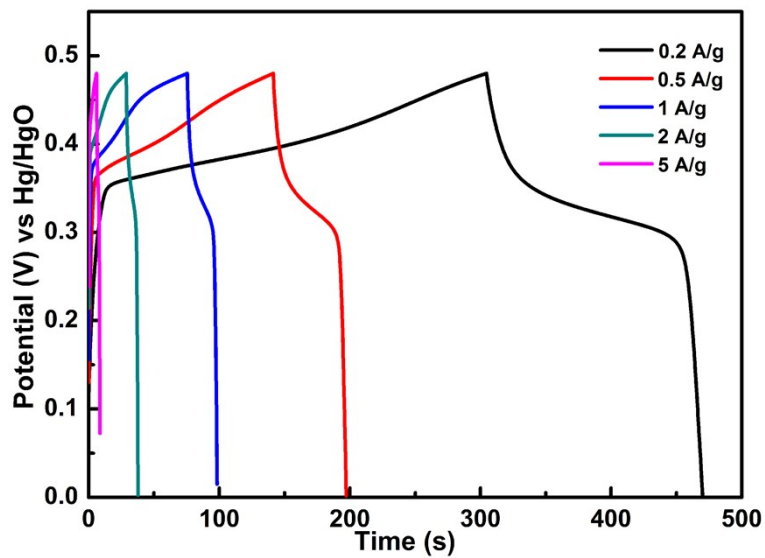


Figure S11. Cyclic voltammetry curves of Co_3O_4 particles measured at different sweep rates.

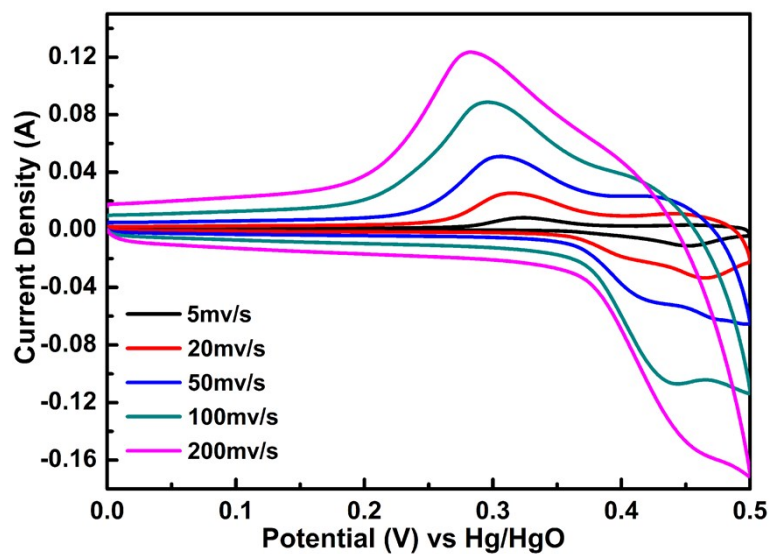


Figure S12. Galvanostatic charge-discharge curves of Co_3O_4 particles at different current densities.

